Al-Azhar Engineering 16th International Conference

Vol. 19, No. 72, July 2024, 1 - 13

RESEARCH ON THE TORSIONAL BEHAVIOR OF PRESTRESSED BEAMS

Mohamed M. sallam*, Amr H. Riad, Hassan, H. El-Esnawi

Civil Engineering Department, Faculty of Engineering, Al-Azhar University, Nasr City, 11884, Cairo, Egypt

***Correspondence:** mohamedsallam698@gmail.com

Citation:

M.M. Sallam, A.H. Riad and H. ElEsnawi, " Researsh on the torsional behavior of prestressed beams" Journal of Al-Azhar University Engineering Sector, vol. 19, pp. 1 - 13, 2024.

Received: 30 October 2023

Revised: 08 December 2023

Accepted: 17 December 2023

DoI:10.21608/auej.2023.248784.1472

ABSTRACT

Prestressed beams are widely used in construction today. Prestressed concrete has several advantages, including enlarging the span of beams, reducing the thickness of buildings, and saving materials compared to regular reinforced concrete. This research demonstrates an experimental program to study the effect of longitudinal tensile stresses as well as the amount of longitudinal reinforcement on prestressed concrete beams under the influence of torsion loads. The behavior of beams is analyzed before, during and after fracture. In this research, seven samples of prestressed beams that were identical in dimensions and characteristics were tested, and the variable were only the longitudinal reinforcement ratio and the pre-Compression stress (P_e/A). After conducting the test, the behavior of the seven beams was analyzed and clarified, which included the crack load and fracture load, twisting angle, torsion moment, deflection curve, stiffness degradation and finally the displacement ductility. It is clear that the maximum load and ductility increased with the increase in longitudinal sidebar. Also, the peak load increased as the Pre-Compression stress (P_e/A) increased. On the other hand, the displacement ductility decreased.

KEYWORDS: Torsion moment, Prestressed concrete beams, Pre-Compression stress.

بحث في السلوك الالتوائي للكمرات سابقة الاجهاد

محمد متولي سلام*، عمرو محمد هلال رياض، حسن حسين الاسناوي

قسم الهندسة المدنية، كلية الهندسة، جامعة الأزهر، مدينة نصر، 11884، القاهرة، مصر.

***البريد الاليكتروني للباحث الرئيسي :** mohamedsallam698@gmail.com

الملخص

تستخدم الكمرات سابقة الإجهاد على نطاق واسع في المباني اليوم. تتمتع الخرسانة سابقة الإجهاد بعدة مميزات، منها زيادة بحور الكمرات، وتقليل سماكة القطاعات الخرسانية، وتوفير المواد مقارنة بالخرسانة المسلحة العادية. يقدم هذا البحث برنامجاً تجريبياً لدراسة تأثير إجهادات الشد الطولية وكذلك نسبة التسليح الطولي على الكمرات الخرسانية سابقة الإجهاد تحت تأثير أحمال الالتواء. يتم تحليل سلوك الكمرات قبل وأثناء وبعد الكسر. تم في هذا البحث اختبار سبع عينات من الكمرات سابقة الإجهاد ومتماثلة في الأبعاد والخصائص، وكان المتغير هو فقط نسبة التسليح الطولي وإجهاد ما قبل الانضغاط ***(P_e/A).*** بعد إجراء الاختبار، تم تحليل وتوضيح سلوك الكمرات السبعة، والتي شملت حمل الشرخ الابتدائي وحمل الكسر، زاوية الالتواء، عزم الالتواء، منحنى الانحراف، الصلابة وأخيراً الممطولية. من الواضح أن الحد الأقصى للحمل والممطولية يزداد مع زيادة التسليح الجانبي الطولي. كما أن الحمل الأقصى يزداد مع زيادة إجهاد ما قبل الضغط ***(P_e/A)*** ومن ناحية أخرى، انخفضت ليونة الممطولية.

الكلمات المفتاحية : عزوم الالتواء، الكمرات سابقة الاجهاد، انضغاط سابق الاجهاد.

1. INTRODUCTION

Prestressed concrete is used in a wide range of buildings and civil structures, where its performance can be improved by enlarging the span of beams, reducing the thickness of buildings, and saving materials compared to regular reinforced concrete. Its typical applications include residential towers, high-rise buildings, bridge and dam structures, foundations, silos and tanks, and nuclear structures. In most concrete structures, pure torsion does not occur frequently and is usually accompanied by bending forces, axial forces, or shear forces [1]. But a torsion study is very important for prestressed beams, especially those used in bridges and beams with wide spans that are subject to loads on one side, for example curved bridges.

The significance of this research is to compensate the lack of knowledge about the behavior of post-tensioned reinforced concrete beams subjected to torsion loading. The effect of some parameters on the torsion strength of pre-stressed reinforced concrete beams was examined. These parameters include the longitudinal reinforcement ratio and tendon pre-stressing force level [2]. Finally, the torsion strength of pre-stressed reinforced concrete beams was predicted and compared with Design Codes.

In the previous Codes, when studying the effect of torsion on prestressed beams, the concrete's resistance to torsion stresses was increased from 0.7 $\sqrt{(f_c)}$ to 0.75 $\sqrt{(f_c)}$. Also, the pre-tension stresses were taken into account in calculating the transverse reinforcement as well as the longitudinal steel through a factor (θ) equal to 45^0 in the case of ordinary beams and beams, the tensile stress is less than 40% of the tensile strength of the bending reinforcement and is equal to 37.50^0 in the case of the tensile stress greater than 40% of the tensile strength of the bending reinforcement [3-7]. The study of the effect of torsion on prestressed beams has not received great importance among researchers, as is the case with the study of bending moments, shear loads, and axial loads. However, there are several studies that have studied the torsion of normal beams and prestressed beams. Three hollow beams were examined and tested till failure [8]. The beams were 5.90 meters long and had a squared cross-section of 0.60 by 0.60 meters. Four wires with a diameter of 1.52 cm that were centered in the cross-section were used to apply external prestressing. For all three beams, the longitudinal reinforcement ratio remained unchanged. After temporary losses, the amount of stress in concrete caused by prestress (f_{cp}) ranged from 0 MPa (beam without prestress) to 3.08 MPa. Tests on the three specimens revealed that longitudinal prestress was useful in delaying cracking and boosting the specimens' resistance to torsion. After cracking, the longitudinal prestress reinforcement begins to function as a regular reinforcement, supporting the internal equilibrium condition of the beams. Also, the behavior of segmental box girders with external prestressing under coupled shear, moment, and torsion was investigated [9]**.** Five specimens total, split into groups I and II for the experiment, were used. Group I investigated the effects of varying load eccentricity at constant pre-stressing force levels (Pe=0.5Pyps) that resulted in torsion levels (e1=0.05m, e2=0.2m, and e3=0.4m). Group II investigated the effects of various tendon pre-stressing forces at constant applied load eccentricity (e3=0.4m), namely Pe=0.5Pyps, Pe=0.38Pyps, and Pe=0.26Pyps. Following the testing program, it was determined that while the ultimate load and ultimate deflection reduced, the maximum twist increased as the applied force eccentricity was raised to increase the torsion effect .Moreover, the linear stage range, ultimate load, ultimate deflection, and ultimate twist all reduced as the effective pre-stressing force rose. Therefore, at the nonlinear stage, the prestressing force level has no effect on the torsional and flexural stiffness of

the beam. Last but not least, raising the effective prestressing strength level significantly improves the beam's resistance to flexure and torsion and delays shear stress cracking. A finite element analysis of the impact of torsion on the structural behavior of externally prestressed monolithic and segmented concrete beams was provided [10]. The results demonstrate that there are notable distinctions between the torsion behavior of segmented and monolithic beams. It was discovered that the primary reason for the nonlinear behavior of EPS beams was openings between segments. For segmental beams, the maximum starting point of nonlinear loads and the final load-carrying capacity are 22% lower than for monolithic beams. Externally prestressed segmental and monolithic beams' load-bearing capability can be significantly impacted by torsion by up to 40%. In comparison to monolithic beams, segmental beams had a maximum twist up to 200% higher at the center. Ultimately, the kind of failure mechanism in an EPS beam is impacted by the presence of torsion. Sliding caused abrupt failures in the segmental beam without torsion [11]. On the other hand, as the twist angle increased, the torsion-beam's stiffness gradually decreased.

2. EXPERAMENTAL INVESTIGATION

Two groups consisting of seven simply supported beams were tested under load up to failure. **Fig. 1** shows the geometry of the beams, supports arrangement, internal reinforcement, and pre-stressing profile of the tested specimens. **Fig. 2** shows the reinforcement cages. The cross-section of all beams was typically R-section with cross-section dimensions 150*400 mm. All beams had the same equal span. All beams were 2300 mm in length, and the supported span was 1800 mm. All the pre-stressing strands with nominal diameters of 15.24 mm comprised 7-wires for fully pre-stressed beams. The first four specimens from Group1 are with variable longitudinal reinforcement ratios. The first specimen (B1) was without longitudinal reinforcement, the other specimens (B2), (B3), and (B4) were with 6Y8, 6T10, and 6T12 longitudinal sidebars respectively. For all specimens, the force in strands was 90 kN (P_e/A=1.50). The transverse reinforcements were closed stirrups Y8@200mm. **Fig. 3** shows details of reinforcement for all specimens. Group2 consists of four specimens with a variable tendon pre-stressing force level. The force in strands was 60, 90, 120, and 150 kN then Pre-Compression stress (P_e/A) were 1.00, 1.50, 2.00, and 2.50 Mpa. The transverse reinforcements were closed stirrups Y8@200mm. The prestressing level is main parameter which prove that it can affected the mode of failure [12]. **Table 1** shows the classification of specimens.

Table 1. The classification of specimens.

Group No	Spec.	Bott RFT	Top RFT	Side. RFT	$\boldsymbol{Pe}$(kN)	$\boldsymbol{P_e/A}$(*Mpa*)	Trans. RFT
Group-1	B1	2Y6	2Y6	---	90	1.50	Y8@200
	B2	2Y6	2Y6	6Y8	90	1.50	Y8@200
	B3	2Y6	2Y6	6T10	90	1.50	Y8@200
	B4	2Y6	2Y6	6T12	90	1.50	Y8@200
Group-2	B5	2Y6	2Y6	6T10	60	1.00	Y8@200
	B3	2Y6	2Y6	6T10	90	1.50	Y8@200
	B6	2Y6	2Y6	6T10	120	2.00	Y8@200
	B7	2Y6	2Y6	6T10	150	2.50	Y8@200

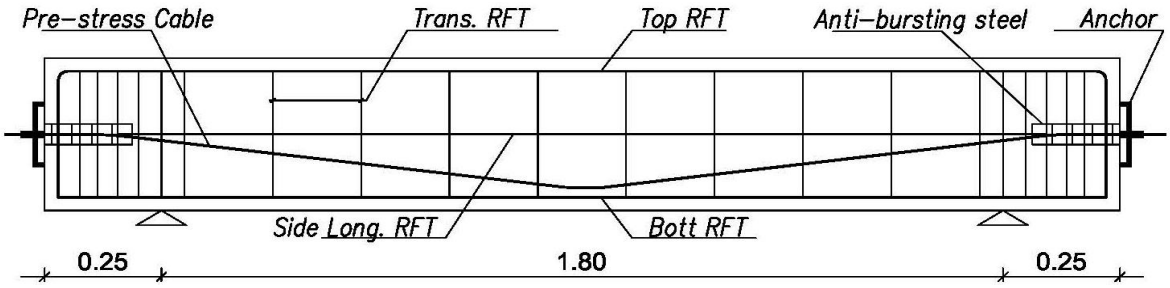

Fig. 1. Details of reinforcement for four specimens.

Fig. 2. Reinforcement cages

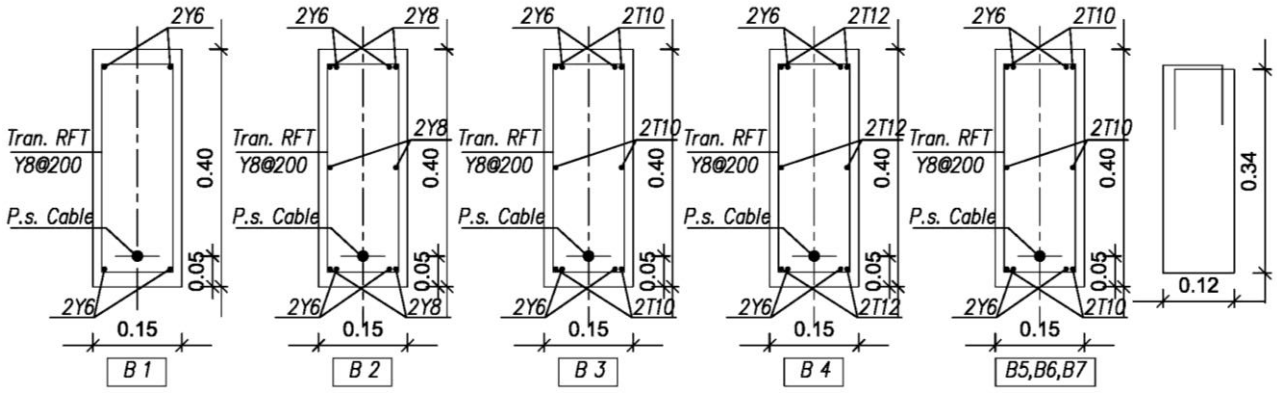

Fig. 3. Details of reinforcement for all specimens.

The average concrete compressive strength for the tested cubes was 39 N/mm2. Two different types of steel reinforcement were used in this research. Normal mild steel with yield strength 334 MPa, and high tensile steel with yield strength 578 MPa. The pre-stressing strands were made of high-grade steel strands comprising seven individual wires each. The strand diameter is 15.24 for fully pre-stressed specimens. The strands were tested in the lab demonstrating the ultimate tensile strength of 1990 MPa. All specimens were tested under constant static load using a hydraulic jack mounted on the steel frame in the R.C. laboratory of the civil engineering department in Al-Azhar University. The specimens were loaded by static load acting at 45 cm from the face of the specimen on a steel cantilever as presented in **Fig. 4**. Steel strains were measured using electrical strain gauges (model KFGS-10-120-C1-11L1M2R). The gauge length was 10.0 mm, its electrical resistance was 119.6±0.40%-ohm, and its gauge factor was 2.09±1.0%, and its transverse sensitivity ratio was 0.1±0.2%, **Fig. 5** shows the arrangement of the steel strain gauges for the specimens. The first strain was placed on the upper side longitudinal bar. The second was placed on the lower side longitudinal bar. Third was placed on mid-side longitudinal bar and the last on the stirrup's branch mid-shear span.

Fig. 4. Experimental setup.

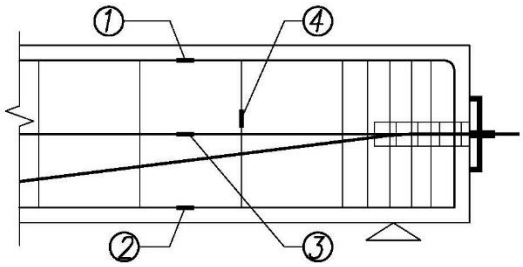

1 – Top long RFT strain

2 – Bottom long RFT strain

3 – Mid. long RFT strain

4 – Transverse RFT strain

Fig. 5. Arrangement of the steel strain gauges for the specimens

3. RESULTS AND DISCUSSION

The results obtained from the experimental tests are torsional Moments – deflection, Torsional Moments-twisting angle curve, Stiffness degradation and displacement ductility [13]. **Fig. 6** shows crack patterns at the failure of the specimen (B1). The first crack was observed at the front left side at a load of 30.0 kN. On the other side, a crack appeared suddenly at load 36 kN, and then the width of the crack was increased without the appearance of other cracks. For specimen B1 the peak load was 40.0 kN and it was obtained at 1.92 mm deflection. **Fig. 7** shows crack patterns at the failure of the specimen (B2). The first crack was observed at the front left side at a load of 31.30 kN, which was bigger than that of the specimen (B1) by 10.0%. The primary crack in this sample occurred then the primary crack increased with the appearance of other cracks other than the specimen (B1) that occurred suddenly. The peak load for the specimen (B2) was 41.72 kN and it was obtained at 3.76 mm deflection It was noted that the peak load of Specimen (B2) was close to Specimen (B1) but the corresponding deflection increased by 29.2%. **Fig. 8** shows crack patterns at the failure of the specimen (B3). The first crack was observed at the front left side at a load of 32.0 kN, which was close to specimen (B1) and specimen (B2). The primary crack in this sample occurred then the primary crack increased with the appearance of other cracks other than the specimen (B1) that occurred suddenly similar to specimens (B2). The peak load for the specimen (B3) was 47.53 kN and it was obtained at 4.48 mm deflection. The peak load of Specimen (B3) was higher than Specimens (B1) and (B2) by 18.80% and 13.93% respectively. The corresponding deflection increased by 39.53% and 7.9% eventually. **Fig. 9** shows crack patterns at the failure of the specimen

(B4). The first crack was observed at the front left side at a load of 31.0 kN, which was close to specimen (B1), specimen (B2) and specimen (B3). The primary crack in this sample occurred then the primary crack increased with the appearance of other cracks other than the specimen (B1) that occurred suddenly similar to specimens (B2) and (B3). The peak load for the specimen (B4) was 49.25 kN and it was obtained at 5.18 mm deflection. The peak load of Specimen (B4) was higher than Specimens (B1), (B2) and (B3) by 23.13%, 18.10%, and 3.61% eventually. The corresponding deflection increased by 170%, 37.76%, and 15.63% respectively.

Fig. 6. Crack patterns at failure of specimen (B1).

Fig. 7. Crack patterns at failure of specimen (B2).

Fig. 8. Crack patterns at failure of specimen (B3)

Fig. 9. Crack patterns at failure of specimen (B4).

From the previous peak loads for the four samples, the relationship between torsional moments and the corresponding deflection can be drawn for Group 1. With the increase of the longitudinal sidebars of the pre-stressed specimen subjected to torsion, the maximum load increases and with the convergence of the primary crack load. Whereas, when adding 6Y8, 6T10, and 6T12 as a longitudinal sidebar, the maximum load was increased by 4.30%, 18.80%, and 23.12% respectively. **Fig. 10** shows Torsional Moments – deflection curve for Group 1.

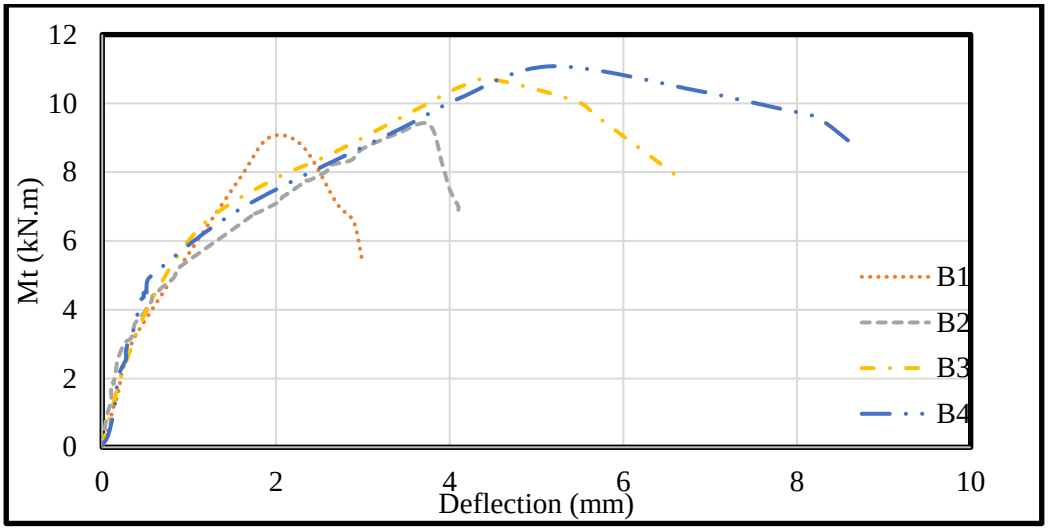

Fig. 10. Torsional Moments – deflection curve for Group 1.

While testing the sample, two LVDTs were placed, one of them under the mid-span of the tested beam and the second under the cantilever at the loading point. The angle of rotation can be measured as the angle of rotation is the landing difference between the two points divided by the distance between them (Δ_2-Δ_1) / L. **Fig. 11** shows the torsional moment – Rotation curve. The angle of rotation at the peak torsional moment was 0.049, 0.061, 0.065, and 0.082 for B1, B2, B3, and B4 eventually. It is clear that the greater the side longitudinal bars of the beam subjected to torsion lead to an increase in the angle of rotation of the specimen at the maximum load. Also, the rotation angle before yield load for the specimen (B4) is higher than that for other specimens.

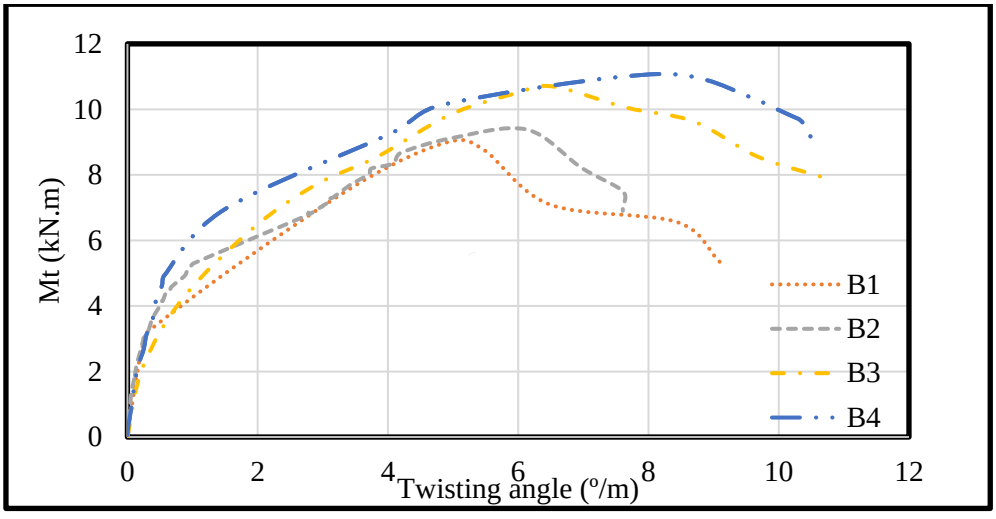

Fig. 11. Torsional Moments - twisting angle curve for Group 1.

Fig. 12 shows the stiffness degradation of the four beams during loading of Group 1. The stiffness of all beams degrades from cracking to yielding but remains almost constant after yielding for specimen that had high longitudinal sidebars. The torsional stiffness of an un-cracked concrete member is not significantly affected by the presence of reinforcement.

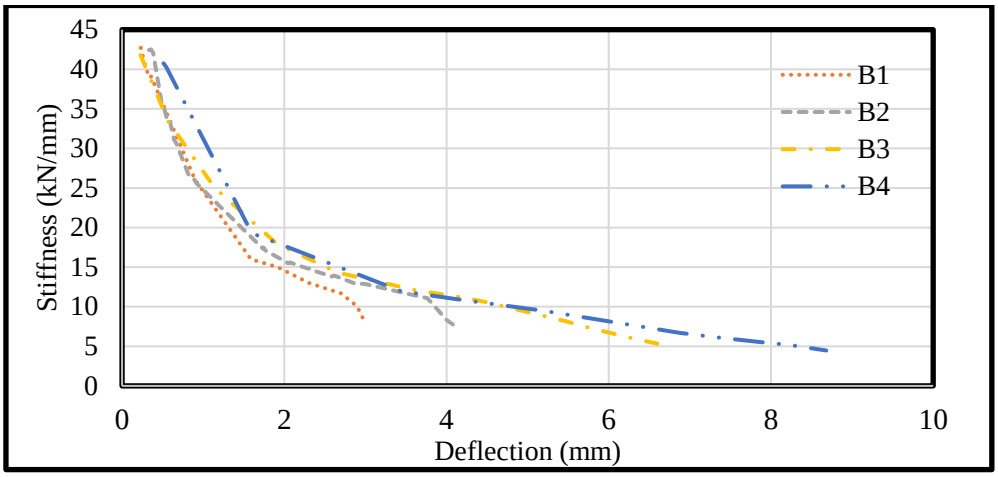

Fig. 12. Deflection-Stiffness curve for Group 1.

Table 2 and **Fig. 13** present the displacement ductility. For specimen (B1) the displacement at peak load was at 1.92 mm and displacement at yield load was at 1.65 mm. It means that the displacement ductility equals 1.17%. Also, when calculating the displacement ductility using the same method for the other three samples, it becomes clear that the displacement ductility equals 1.35% for specimen (B2), 1.70% for specimen (B3) and 1.73% for specimen (B4). So, the displacement ductility of specimens B2, B3, and B4 are 15.39 %, 45.30%, and 47.86% higher than B1 respectively. These values indicate that the specimen without sidebars is the least in the ductility value. As for the other three specimens, with the increase of the sidebars, the ductility increases.

Table 2. Ductility displacement of specimens of Group 1.

Specimen	Side Bars	Yield displacement(mm)	Ult. displacement(mm)	Ductility index (%)
B1	-	1.65	1.92	1.17
B2	6Y8	2.80	3.76	1.35
B3	6T10	2.65	4.48	1.70
B4	6T12	3.00	5.18	1.73

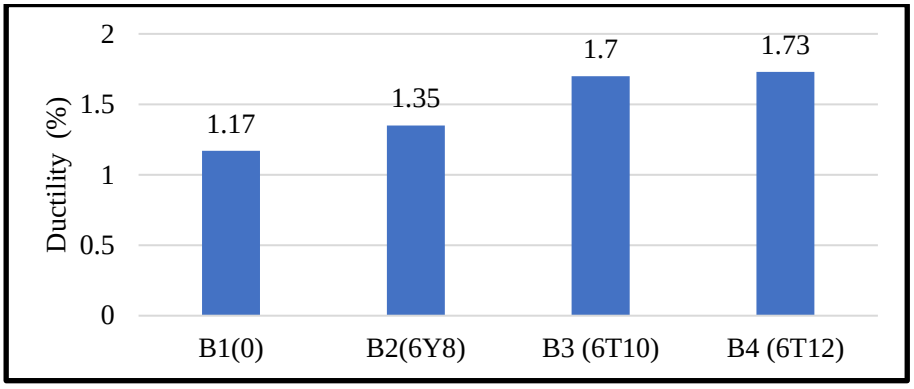

Fig. 13. Displacement ductility for Group 1.

For Group 2, **Fig. 14** shows crack patterns at failure of specimen (B5). The first crack was observed on both sides at load 30 kN. For specimen (B5) the peak load was 44.53 kN and it was at 4.22 mm displacement. It was previously explained the shape of the crack, crack load, and peak load for specimen (B3). By comparing it with specimen (B5), it is clear that the peak load of Specimen (B3) was higher than Specimens (B5) by 6.73%. **Fig. 15** shows crack patterns at failure of specimen (B6). The first crack was observed at the front left side at load 32 kN, which was bigger than that of specimen (B5). On the right side, the first crack was observed at 33 kN. The primary crack in this sample occurred then the primary crack increased with the appearance of other cracks similar to specimen (B5). The peak load for the specimen (B6) was 53.82 kN and it was at 6.70 mm displacement. It was noted that the peak load of Specimen (B6) was higher than Specimens (B5) and (B3) by 20.86% and 13.32% respectively. **Fig. 16** shows crack patterns at failure of specimen (B7). The first crack was observed at the front left side at load 38 kN, which was higher than that of specimen (B5), (B3), and (B6) by 26%, 18.75%, and 18.75% respectively. The peak load for specimen (B4) was 57.61 kN and it was at 9.77 mm displacement. The peak load of Specimen (B7) was higher than Specimens (B5), (B3) and (B6) by 29.73%, 21.21%, and 7.04% eventually. The corresponding deflection increased by 6.16%, 58.77%, and 131.5% respectively.

Fig. 14. Crack patterns at failure of specimen (B5).

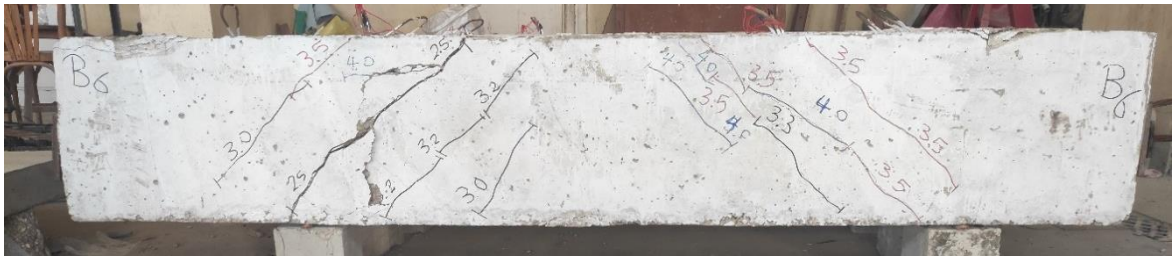

Fig. 15. Crack patterns at failure of specimen (B6).

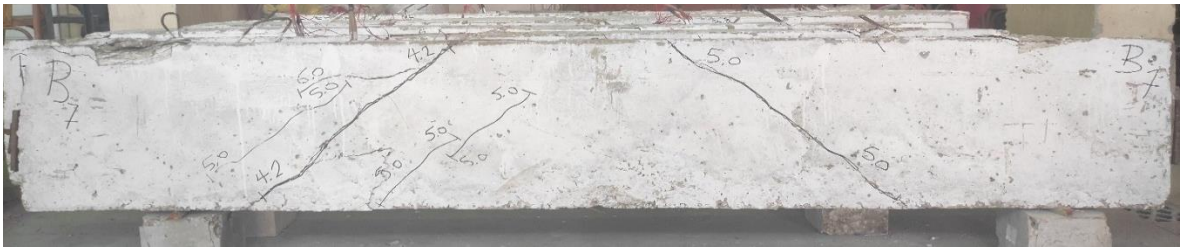

Fig. 16. Crack patterns at failure of specimen (B7).

Fig. 17 shows torsional moment versus mid-span deflection responses of all tested beams in Group 2. An increasing Pre-Compression stress (P_e/A) resulted an increasing in peak load by 59.42%, 29.73%, and 26.20% respectively. Where the peak torsional moment for four specimens was 10.02 kN.m, 10.69 kN.m, 12.11 kN.m, and 12.96 kN.m respectively.

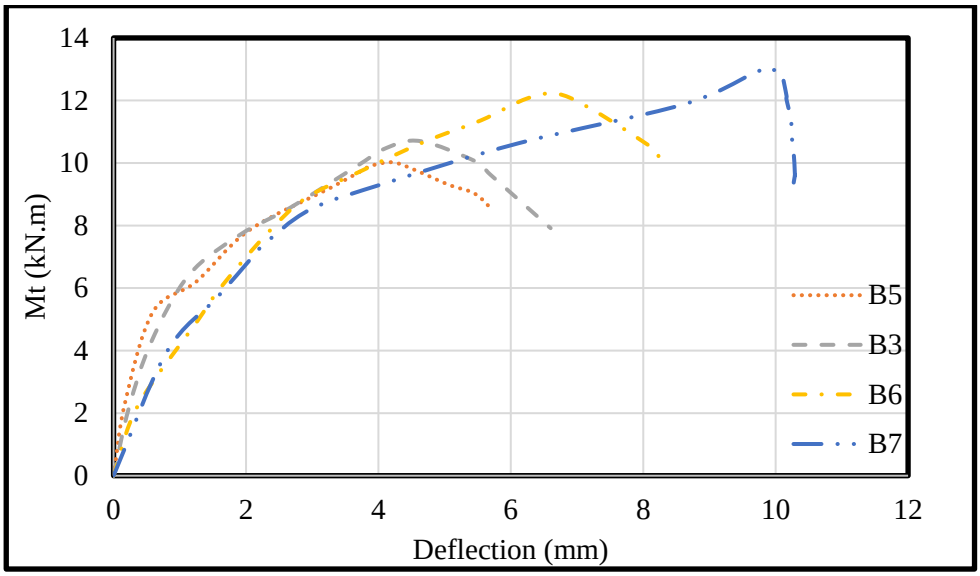

Fig. 17. -Torsional Moments – deflection curve of tested beams in Group 2.

Fig. 18 shows torsional moment – Rotation curve for Group 2. The angles of rotation at peak load were 0.052, 0.065, 0.064, and 0.077 for B5, B3, B6, and B7 eventually. The greater tendon pre-stressing force level of beam subjected to torsion leads to an increase in the angle of rotation of specimen at the maximum load but the rotation angle before yield load for all specimens was close.

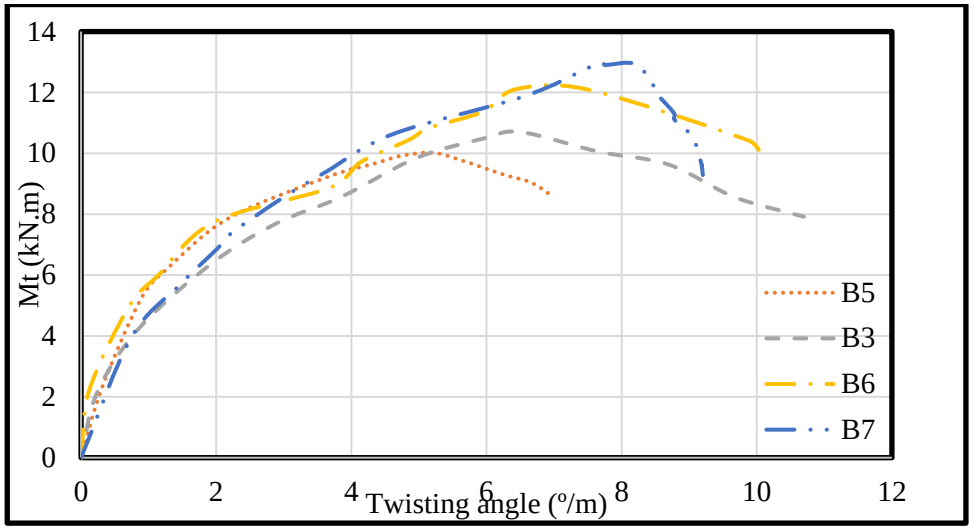

Fig. 18. Torsional Moments – twisting angle curve in Group 2.

Fig. 19 shows stiffness degradation of the four beams during loading of Group 2. The stiffness of all beams degrades from cracking to yielding. The initial stiffness degradation for specimens B6 and B7 was higher than specimens B5 and B3 but remains almost constant after yielding for specimens B6 and B7 than that for specimens B5 and B3. It can be concluded from the Figure that high tensile strength in the cable leads to fast stiffness degradation. After yield load, the curve remains constant, unlike specimens with low tensile strength in the cable. It is noticeable that the stiffness of the specimens with lower cable strength is higher than the other specimens until the yield load and then the opposite happened as the stiffness of samples with lower strength decreased quickly than the other specimens.

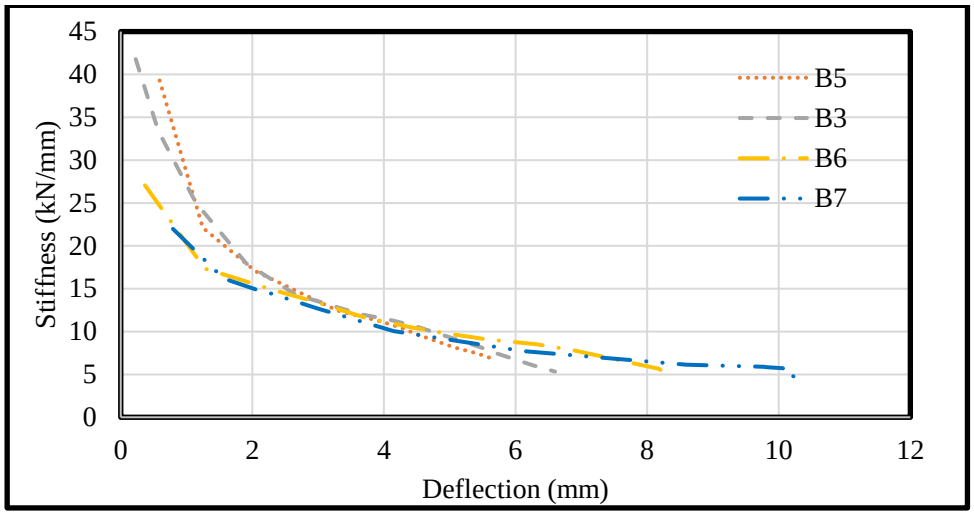

Fig. 19. Deflection-Stiffness curve for Group 2.

Table 3 and **Fig. 20** present the displacement ductility for the test specimen of Group 2. For specimen (B5) the displacement at peak load was 4.22 mm and displacement at yield load was 2.40 mm. It means that the displacement ductility equals 1.76%. For specimen (B6) the displacement at peak load was 6.70 mm and displacement at yield load was 4.00 mm. It means that the displacement ductility equals 1.68%. For specimen (B7) the displacement peak load was obtained 9.77 mm, displacement at yield load was obtained 6.50 mm. It means that the displacement ductility equals

1.51%. So, the displacement ductility of specimens B3, B6, and B7 are 3.41 %, 4.55%, and 14.20% lower than B5 respectively. These values indicate that the displacement ductility decrease with the increase Pre-Compression stress (P_e/A).

Table 3: Ductility displacement of specimens of Group 2.

Specimen	Force (kN)	Y. displacement (mm)	Ult. Displacement (mm)	Ductility index (%)
B5	60	2.40	4.22	1.76
B3	90	2.65	4.48	1.70
B6	120	4.00	6.47	1.68
B7	150	6.50	9.77	1.51

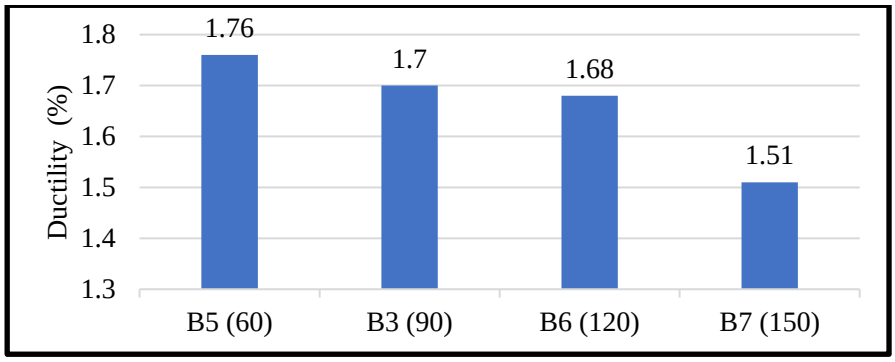

Fig. 20. Displacement ductility for Group 2.

4. CONCLUSIONS

At the end, the following is concluded:

- With the increase of longitudinal sidebars of pre-stressed specimen subjected to torsion, the maximum load increases and with the convergence of primary crack load. Whereas, when adding 6Y8, 6T10, and 6T12 as a longitudinal sidebar, the maximum load was increased by 4.30%, 18.80%, and 23.12% respectively.
- It was noted that the longitudinal sidebars help to distribute the cracks, as the specimen without longitudinal sidebars had one crack and then increased in width. Unlike other samples that had longitudinal sidebars, several cracks appear on both sides. And it is noted that the longitudinal sidebars did not delay the primary crack.
- The longitudinal sidebars of the specimen improve the stiffness and ductility of the specimen. Whereas, when adding 6Y8, 6T10, and 6T12 as a longitudinal sidebar, the displacement ductility was increased by 15.39 %, 45.30%, and 47.86% respectively
- With the increase in Pre-Compression stress (P_e/A), the resistance of the sample to torsion increases by a large percentage, and the primary crack also occurs at a higher load. Whereas, with increasing the Pre-Compression stress (P_e/A) from 1.00 Mpa to 1.50, 2.00, and 2.50 Mpa, the peak load increased by 6.70%, 20.80%, and 29.73% respectively.

- With the increase in Pre-Compression stress (P_e/A), the ductility of the sample decreases. Whereas, with increasing the Pre-Compression stress (P_e/A) from 1.00 Mpa to 1.50, 2.00, and 2.50 Mpa, the displacement ductility decreases by 3.41 %, 4.55%, and 14.20% respectively.
- The stiffness of the specimens with lower Pre-Compression stress (P_e/A) is higher than the other specimens until the yield load, then the opposite happened as the stiffness of the specimens with lower Pre-Compression stress (P_e/A) decreased quickly than the other specimens.

References

[1] - Onsongo, W. M., "The Diagonal Compression Field Theory for Reinforced Concrete Beams Subjected to Combined Torsion, Flexure, and Axial Load," Ontario, Canada, 1978, 246 pp.

[2] - Mardukhi, J., "The Behavior of Uniformly Prestressed Concrete Box Beams in Combined Torsion and Bending," Canada, 1974, 73 pp.

[3] - ACI Committee 318, "Building Code Requirements for Structural Concrete (ACI 318-05) and Commentary (318R-05)," American Concrete Institute, Farmington Hills, MI, 2005, 430 pp.

[4] - CSA-A23.3-04, "Design of Concrete Structures," Canadian Standards Association, Rexdale, Ontario, Canada, 2004.

[5] - Egyptian code committee 203: Egyptian code of practice for design and construction of reinforced concrete structures, housing and building research center, Cairo, 2020.

[6] - British Standards Institution. BS 8110 Part 1: structural use of concrete: code of practice for design and construction. London: BSI; 1997.

[7] - Eurocode 2, "Design of Concrete Structures—Part 1-1: General Rules and Rules for Buildings," CEN, EN 1992-1-1, Brussels, Belgium, 2004,225 pp.

[8] – Luís, B., Sérgio, L., Mafalda, T., "Experimental study on the torsional behavior of prestressed HSC hollow beams" applied science, MDPI, 2020.

[9] - El-Shafiey, T, "Experimental investigation on the behavior of segmental box girder bridges with external prestressing under combined shear, moment and torsion" ICASGE'17 27-30 March 2017, Hurghada, Egypt.

[10] - Al-Gorafi, M.A, "Externally Prestressed Monolithic and Segmental Concrete Beams under Torsion: A Comparative Finite Element Study" IOP Conf. Ser.: Mater. Sci. Eng. 17 012041, 2011.

[11] - Elharouney, B. H., Hussein, A., Mostafa, E., and Elnemr, "Flexural behavior of prestressed concrete beams strengthened by near surface mounted FRP rods" A., Journal of Al-Azhar University Engineering Sector Vol. 14, No. 53, October, 2019, 1424-1435.

[12] - Huang, T., "Influence of prestress level on shear behavior of beams," Tech. Pap., vol. 31, no. 2, 2009.

[13] - Bernardo, L.F.A.; Lopes, S.M.R. Torsion in HSC Hollow Beams: Strength and Ductility Analysis. ACI Struct.J. 2009, 106, 39–48.